Design and Development of a Novel Humidity-Tolerant Gas Sensing Material for Reliable and High-Performance Ethanol Detection

Dongting Wang [1, a, b], Shan Ding [1, a], Su'e Chen [b], Dongyu Shan [c], Xinning Zhang [d,*], Chunjie Jiang [a,*]

[a] *School of Chemistry and Chemical Engineering, Liaoning Normal University, Dalian 116029, PR China.*

[b] *Department of Science and Environmental Studies, The Education University of Hong Kong, Hong Kong SAR, China*

[c] *Liaoning Provincial Ecology & Environment Monitoring Center, Shenyang 110161,PR China*

[d] *School of Materials Science and Engineering, Peking University, Beijing 100871, China*

* Corresponding authors. Tel/fax: +86 411 82156708; E-mail address: jiangcj@lnnu.edu.cn (C. Jiang).

* Corresponding authors. Tel/fax: 0411-82156708

E-mail address: jiangcj@lnnu.edu.cn (C. Jiang)

[1] These authors contributed equally to this work.

1. Materials

Tin(IV) chloride pentahydrate ($SnCl_4 \cdot 5H_2O$, AR) and antimony(III) chloride ($SbCl_3$, AR) were purchased from Aladdin Chemical Co., Ltd. (Shanghai, China). Polyvinylpyrrolidone (PVP K30, AR) was obtained from Aladdin Chemical Co., Ltd. (Shanghai, China). Hydrochloric acid (HCl, AR) and ethanol (AR) were obtained from Sinopharm Chemical Reagent Co., Ltd. (Shanghai, China). Chloroplatinic acid (H_2PtCl_4, AR) and sodium borohydride ($NaBH_4$, AR) were provided by Aladdin Chemical Co., Ltd. (Shanghai, China). All chemicals were used directly without further purification. Deionized water (about 18.2 MΩ·cm) was produced by a KSV Minitrough system.

2. Instruments

X-ray diffraction (XRD, D8 ADVANCE DAVINCI, Germany) was used to examine the crystal properties of the materials. Morphologies and microstructure compositions were observed using scanning electron microscopy (SEM, Hitachi S4800, Japan) and transmission electron microscopy (TEM, JEOL2100, Japan) / high-resolution transmission electron microscopy (HRTEM, Tecnai F20, USA). Surface area was measured by Brunauer–Emmett–Teller (BET, ASAP2020M, USA), and pore size distribution was analyzed by Barrett–Joyner–Halenda (BJH, ASAP2020M, USA). The oxidation states of surface species were identified using X-ray photoelectron spectroscopy (XPS, Axis Ultra DLD, UK).

3. Fabrication of Gas Sensor and Testing schematic

The sensor fabrication follows the same method described in our previous study, illustrated in Figure 1(a) . Initially, a Ni-Cr heating wire is inserted into a ceramic tube, and four platinum wires are soldered to the Ni-Cr wire on a six-legged base, with any surplus lead wires trimmed off. Then, the sensitive material is mixed with distilled water at a volume ratio of 1:4 in a mortar and ground until a uniform paste is formed. This mixture is applied evenly onto the outer surface of the ceramic tube. The assembly is dried in an oven at 150 °C for 2 hours. After drying, an appropriate explosion-proof mesh is firmly fixed onto the six-legged base. Finally, the sensor undergoes an aging process on an aging table at a constant current of 70 mA for 24 hours to stabilize its resistance at room temperature (25°C). Gas sensing measurements were performed using the cGs-8 gas sensors, as shown in Figure 1(b) and testing schematic are presented in Figure 1(c) .

The schematic diagram of the n-type metal oxide semiconductor illustrates the adsorption of oxygen molecules on its surface, where these molecules capture free electrons to form oxygen ions (e.g., O_2^-). This electron capture results in a decrease of free electron concentration near the surface, causing band bending to occur.

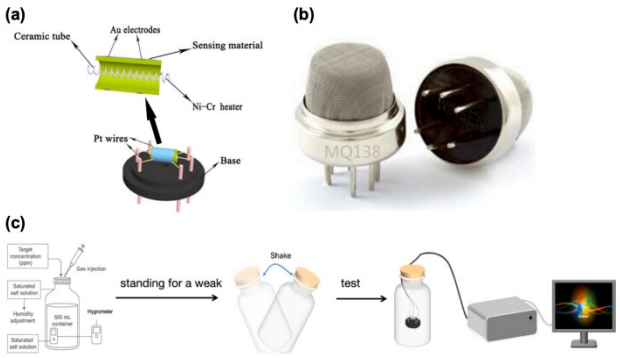

Figure. S1. (a) Schematic diagram of the gas sensor. (b) Schematic Diagram of a Gas Sensor Probe. (c) Schematic diagram of gas preparation under different humidity conditions and testing schematic.

4. Gas Preparation:

1 Determine the target gas concentration：

Identify the desired gas concentration (in ppm) in the 500 mL container according to your experimental requirements.

2 Calculate the gas volume：

Calculate the required gas volume using the formula:

Volume (mL) = Target Concentration (ppm)×Container Volume (mL)×10^{-6}.

3 Set the humidity level：

Add moisture to the container using a humidifier or water vapor generator, continuously monitoring and adjusting with a hygrometer until the desired relative humidity (RH) is reached.

4 Humidity control method：

Place saturated salt solutions with known equilibrium humidity inside a sealed container and leave it at room temperature for about one week to allow the humidity to stabilize. Common saturated salt solutions and their corresponding equilibrium relative humidity (RH) are: lithium chloride (LiCl) solution for approximately 11% RH, magnesium chloride ($MgCl_2$) solution for about 33% RH, sodium bromide (NaBr) solution for around 55% RH, potassium chloride (KCl) solution for about 74% RH, and sodium sulfate (Na_2SO_4) solution for approximately 95% RH. Use a humidity sensor to measure the RH inside the container to confirm that the humidity has stabilized and meets the expected values.

Relative humidity (RH) is defined as the ratio of the partial pressure of water vapor in the air (P_{H2O}) to the equilibrium vapor pressure of water at the same temperature ($P_{H2O, sat}$)

$$RH\ (\%) = \frac{P_{(H2O)}}{P_{(H2O,\ sat)}} \times 100\%$$

RH is highly temperature-dependent; for a constant amount of water vapor, an increase in temperature leads to a decrease in RH because the saturation vapor pressure increases.

5 Calculate the volume of gas source：

Use the ideal gas law PV = nRT to calculate the required moles of gas. Considering that one mole of gas occupies approximately 24 L at room temperature and atmospheric pressure, convert this to the mass and volume of the volatile liquid gas source based on its molecular weight and density.

Tab. S1. Injection Volume of Volatile Liquids

Gas Type	Molecular Weight (g/mol)	Density (g/mL)	Liquid Volume (μL)	Purity (%)
Ethanol	46.07	0.789	0.122	>99.7 (analytical grade)
Methanol	32.04	0.792	0.084	>99.9 (analytical grade)
Acetone	58.08	0.784	0.154	>99.5 (analytical grade)
Benzene	78.11	0.879	0.184	>99.5 (analytical grade)
Toluene	92.14	0.867	0.221	>99.8 (analytical grade)
Xylene	106.17	0.861	0.257	>99.0 (analytical grade)

6 Mixing and verification：

After determining the required gas volume, seal the container and gently shake it to ensure homogeneous mixing of gas and moisture.

Finally, verify the humidity and gas concentration with appropriate sensors to confirm they meet the experimental requirements.

The sensor operating temperature was set at 100°C (T_{op}=100°C), while the relative humidity was defined and controlled at 25°C (T_{test}=25°C) using saturated salt solutions. All measurements were conducted under ambient pressure (P_{op}=P_{test}=1atm). No high-pressure chamber was involved.

5. Gas sensing properties

Tab. S2 Response of the SnO_2 gas sensor to 100 ppm ethanol in 20 days.

First Response																	
		11%RH		33%RH			55%RH			74%RH			95%RH				
		response	response time (s)	recovery time (s)	response	response time (s)	recovery time (s)	response	response time (s)	recovery time (s)	response	response time (s)	recovery time (s)	response	response time (s)	recovery time (s)	response	response time (s)	recovery time (s)
0%Sb	0% Pt	55	2	112	25	2	123	20	3	139	19	4	154	17	4	162			
	2% Pt	65	2	114	33	3	132	23.3	3	144	16	3	150	15	3	163			
	4% Pt	77	2	121	35	2	129	19	3	136	17	4	149	15.4	4	159			
	6% Pt	85	2	123	43	2	133	21	2	139	19	4	152	16.3	4	164			
	8% Pt	73	1	125	37	2	131	17	2	142	12	3	147	12	4	161			
2%Sb	0% Pt	23.5	2	116	23	3	143	23.3	4	145	22.9	3	144	23	3	164			
	2% Pt	25	2	119	24	3	141	23.6	3	142	23.3	3	141	22.8	4	166			
	4% Pt	28	3	121	26	4	145	25	4	148	23	4	139	22	5	161			
	6% Pt	32	2	131	31.5	3	151	30	3	146	28	4	137	26	4	168			
	8% Pt	29	2	130	25	2	139	20	3	151	18	3	144	15	4	159			
4%Sb	0% Pt	30	2	118	31.5	2	144	31	3	156	30	3	156	30.8	4	157			
	2% Pt	33	2	124	32.5	2	141	32	4	150	32.3	3	155	32.6	3	159			
	4% Pt	35	2	131	35.2	3	139	35.5	3	149	34.9	4	160	34.7	4	162			
	6% Pt	38	2	137	36	3	147	35	3	156	33	3	149	32	4	166			
	8% Pt	41	2	132	37	2	151	35.5	4	159	28	3	146	24	4	161			
6%Sb	0% Pt	23.5	3	125	23	2	156	23.3	5	151	22.9	3	165	23	2	161			
	2% Pt	19	4	126	19.6	2	151	19	4	155	20.1	3	162	18.9	3	163			
	4% Pt	30	4	121	31.5	3	159	31	3	159	30	4	160	30.8	3	168			
	6% Pt	42.3	2	133	42.5	3	161	42	3	161	42.4	3	156	42.5	3	166			
	8% Pt	29	3	131	25	2	166	20	3	158	18	3	151	15	2	161			
8%Sb	0% Pt	29	3	136	25	4	154	20	3	159	18	2	161	15	3	169			
	2% Pt	29.5	3	131	30.1	3	155	29	3	166	28.6	3	168	26	3	171			
	4% Pt	31	4	134	30.5	2	157	29.8	2	161	30	2	166	29.8	4	166			
	6% Pt	35	4	142	34.5	3	149	34.6	3	150	34	3	161	34.4	3	164			
	8% Pt	44	3	137	38	2	155	34	3	168	32	3	159	29	3	167			

Repeatability Response (20 cycles)																	
		11%RH			33%RH			55%RH			74%RH			95%RH			
		response	response time (s)	recovery time (s)	response	response time (s)	recovery time (s)	response	response time (s)	recovery time (s)	response	response time (s)	recovery time (s)	response	response time (s)	recovery time (s)	
0%Sb	0% Pt	53	2	124	23	2	122	19	5	141	19	3	154	17	3	163	
	2% Pt	64	2	121	34	2	131	24	3	146	17	3	149	15	2	159	
	4% Pt	78	2	116	34	2	133	19	2	139	17	3	141	15.4	3	155	
	6% Pt	88	1	122	43	2	141	22	3	137	19	2	151	16.3	3	161	
	8% Pt	74	1	130	37	2	133	16	2	140	13	2	147	13	3	160	
2%Sb	0% Pt	24	3	122	22	3	142	24	4	144	24	4	167	23	2	153	
	2% Pt	25	2	121	24	2	131	23	2	141	23.3	3	155	23	3	147	
	4% Pt	27	3	114	27	3	129	26	3	139	24	2	158	21	3	151	
	6% Pt	31	2	119	31.5	2	128	31	3	137	27	2	149	27	2	144	
	8% Pt	28	2	115	26	2	133	20	3	143	19	3	161	14	2	149	
4%Sb	0% Pt	31	3	131	31.5	4	154	31	3	159	31	3	144	31	4	171	
	2% Pt	33	2	140	32	3	138	33	3	155	33	3	141	33	2	160	
	4% Pt	34	2	133	34	2	142	35.5	2	151	34	4	139	35	3	165	
	6% Pt	39	3	129	37	3	155	36	2	161	33	3	147	32	3	159	
	8% Pt	41	1	127	37	3	144	37	2	163	29	2	142	23	2	166	
6%Sb	0% Pt	24	2	133	24	3	159	18	5	162	24	3	153	24	3	169	
	2% Pt	19	3	141	21	2	141	18	3	165	22	3	151	19	2	171	
	4% Pt	31	2	139	33	3	149	30	3	167	31	4	144	30.8	3	166	
	6% Pt	44	2	133	42.5	3	146	42	3	159	43	3	153	42.5	3	162	
	8% Pt	30	1	129	24	3	150	21	3	157	18	2	149	16	3	160	

Table S2 summarizes the corresponding response and recovery times of these sensors under identical humidity conditions. After 20 days of continuous testing, the 6 wt% Pt/6% Sb–SnO_2 sensor maintained excellent stability (response ≈ 43) and strong humidity tolerance, together with relatively stable response and recovery times.

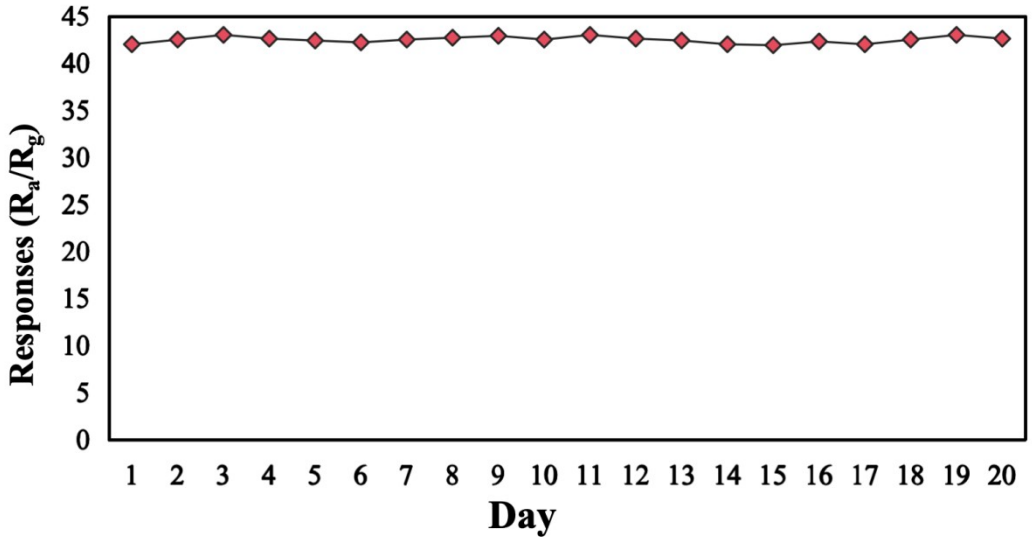

Figure S2. Response of the 6 wt% Pt/6% Sb–SnO_2 to 100 ppm methanol in 20 days.

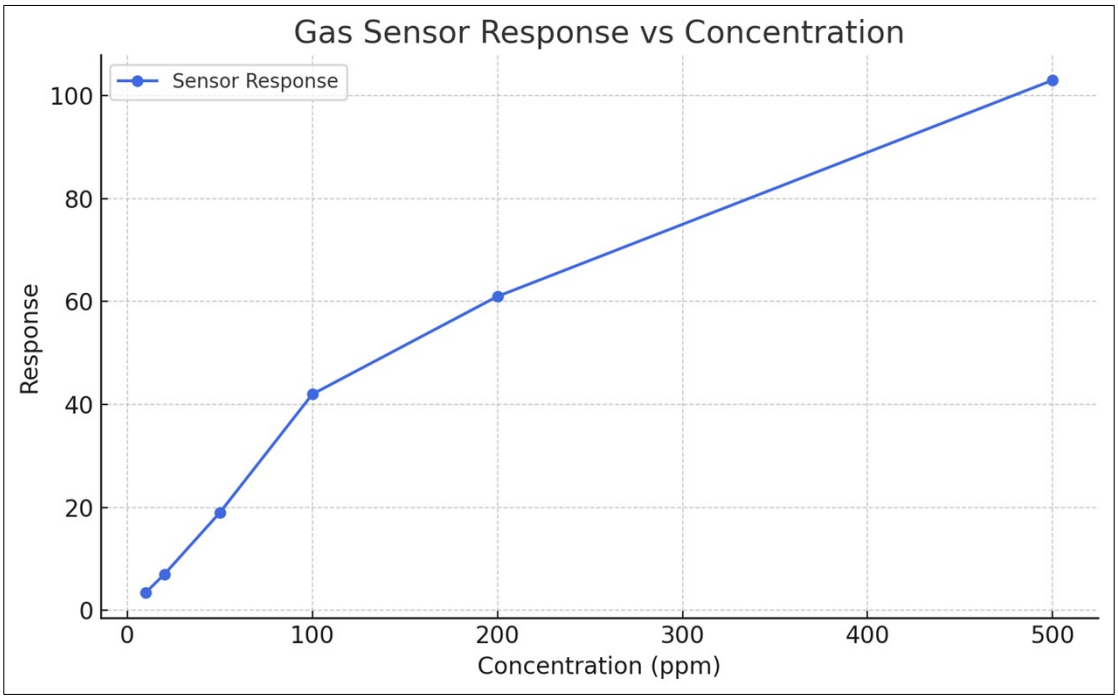

Figure S3. Sensor response as a function of ethanol concentration with estimated detection limit (LOD).

To assess the sensor's sensitivity to ethanol, response tests were conducted at various ethanol concentrations. According to the empirical formula $R=K[Q]+R_0$, where R and R_0 represent the response value after introducing ethanol gas and the baseline response value, respectively, [Q] is the ethanol concentration, and K is the sensitivity constant. Linear fitting results show that the response value (res) and ethanol concentration (ppm) are related by $res=0.198\times[ppm]+10.17$. The sensor's detection limit can be calculated using the formula $LOD=3\sigma/K$, where σ is the standard deviation of repeated measurements in air, and K is the slope of the linear fit (sensitivity), which is 0.198 in this case, as shown in Figure S3. Substituting these values yields a detection limit of approximately 7.57 ppm.

Tab. S3: Comparison of State-of-the-Art Humidity-Tolerant Ethanol Sensors

Structures	Working Temperature (°C)	Concentration (ppm)	Gas Response (Ra/Rg)	Response/Recovery Time (s)	Relative Humidity	Ref.
SnO_2 nanotubes	300	200	16.7	7	30%	[S1]
SnO_2@ZnO nano spheres	270	50	7.5	1.2	33%	[S2]
1 mol% W-doped CeO_2 hollow nanofibers	200	100	10.2	7.04/55.30	Humidity-independent	[S3]
PTFE/Au/WO_3 composite films	220	100	17.1	7/5	30–90% RH (high retention)	[S4]
SnO_2 nanowires	360	100	31	1 – 10	Dry air	[S5]
Hollow SnO_2 NPs	300	100	29.2	2	98%	[S6]
RGO-SnO_2 nanocomposite	300	100	43.0	8	98%	[S7]
SnO_2 nanoflowers	300	100	47.29	10	Dry air	[S7]
6 wt% Pt/6% Sb–SnO_2	100	100	42	3/161	Humidity-independent	this work

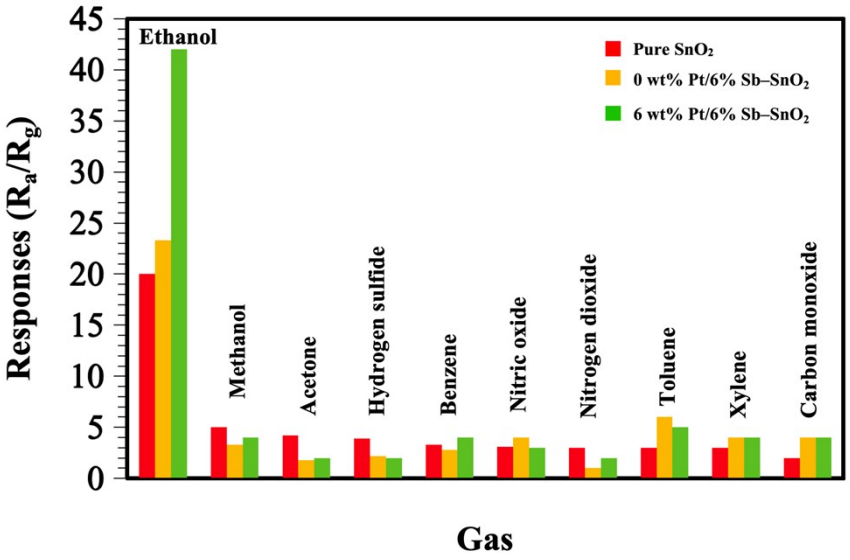

Figure S4. Response of a pure SnO_2 gas sensor, 0 wt% Pt/6% Sb–SnO_2 sensor, 6 wt% Pt/6% Sb–SnO_2 sensor to 100 ppm different gas at 100°C.

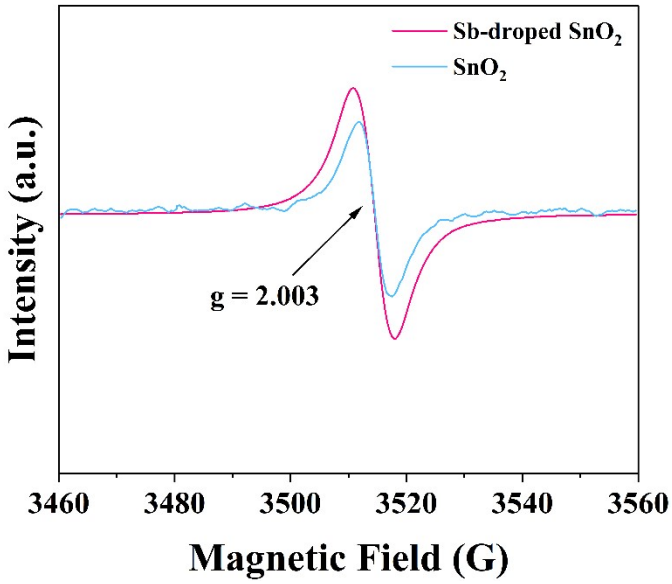

Figure S5. EPR spectra of pure SnO_2 and Sb-doped SnO_2 samples.

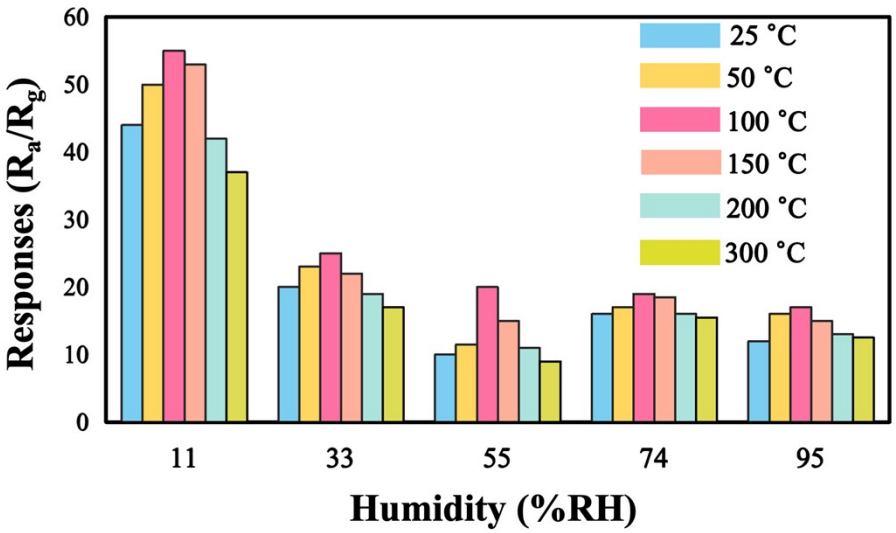

Figure S6. Response of 6 wt% Pt/6% Sb–SnO_2 to 100 ppm ethanol under different humidity conditions at different temperature (T_{test}=25°C, P_{op}=P_{test}=1atm).

References：

[S1] J. Zhang, J. Guo, H. Xu, B. Cao, Reactive-template fabrication of porous SnO_2 nanotubes and their remarkable gas-sensing performance, *ACS Appl. Mater. Interfaces* 5 (2013) 7893–7898, http://dx.doi.org/10.1021/am4019884.

[S2] R. Zhang, T. Zhou, L. Wang, Z. Lou, J. Deng, T. Zhang, The synthesis and fast ethanol sensing properties of core–shell SnO_2@ZnO composite nanospheresusing carbon spheres as templates, *New J. Chem.* 40 (2016) 6796–6802, http://dx.doi.org/10.1039/C6NJ00365F.

[S3] Wang, X., Wang, X., Wei, W., Jiang, H., Li, X., Liu, G., … Zhang, Z. (2023). Humidity-resistant ethanol gas sensors based on electrospun tungsten-doped cerium oxide hollow nanofibers. *Sensors and Actuators B: Chemical,* 393, 134210. https://doi.org/10.1016/j.snb.2023.134210

[S4] Zhu, X., Chang, X., Jiang, Y., Gao, W., & Sun, S. (2025). Hydrophobicity-promoted humidity-resistant ethanol sensors based on PTFE/Au/WO_3 composite films. *Sensors and Actuators B: Chemical,* 430, 137386. https://doi.org/10.1016/j.snb.2025.137386

[S5] S. Phadungdhitidhada, S. Thanasanvorakun, P. Mangkorntong, S. Choopun, N. Mangkorntong, D. Wongratanaphisan, SnO_2 nanowires mixed nanodendrites for high ethanol sensor response, *Curr. Appl. Phys.* 11 (2011) 1368–1373, http://dx.doi.org/10.1016/j.cap.2011.04.007.

[S6] Zito, C. A., Perfecto, T. M., & Volanti, D. P. (2017). Impact of reduced graphene oxide on the ethanol sensing performance of hollow SnO_2 nanoparticles under humid atmosphere. *Sensors and Actuators B: Chemical,* 244, 466-474.

[S7] X. Yu, W. Zeng, Fabrication and gas-sensing performance of nanorod-assembled SnO_2 nanostructures, *J. Mater. Sci. Mater.* Electron. 27 (2016) 1–6, http://dx.doi.org/10.1007/s10854-016-4721-0.